Small-Molecule Inhibitors of SETD8 with Cellular Activity

Gil Blum,[†,‡,⊥] Glorymar Ibáñez,[†,§,⊥] Xiangjun Rao,[∥] David Shum,[§] Constantin Radu,[§] Hakim Djaballah,[†,§] Judd C. Rice,[∥] and Minkui Luo*[,†]

[†]Molecular Pharmacology and Chemistry Program, [‡]Tri-Institutional Training Program in Chemical Biology, and [§]HTS Core Facility, Memorial Sloan Kettering Cancer Center, New York, New York 10065, United States

[∥]Department of Biochemistry and Molecular Biology, University of Southern California Keck School of Medicine, Los Angeles, California 90089, United States

S Supporting Information

ABSTRACT: SETD8/SET8/Pr-SET7/KMT5A is the sole protein lysine methyltransferase (PKMT) known to monomethylate lysine 20 of histone H4 *in vivo*. SETD8's methyltransferase activity has been implicated in many essential cellular processes including DNA replication, DNA damage response, transcription modulation, and cell cycle regulation. Developing SETD8 inhibitors with cellular activity is a key step toward elucidating the diverse roles of SETD8 via convenient pharmacological perturbation. From the hits of a prior high throughput screen (HTS), **SPS8I1−3** (NSC663284, BVT948, and ryuvidine) were validated as potent SETD8 inhibitors. These compounds contain different structural motifs and inhibit SETD8 via distinct modes. More importantly, these compounds show cellular activity by suppressing the H4K20me1 mark of SETD8 and recapitulate characteristic S/G2/M-phase cell cycle defects as observed for RNAi-mediated SETD8 knockdown. The commonality of **SPS8I1−3** against SETD8, together with their distinct structures and mechanisms for SETD8 inhibition, argues for the collective application of these compounds as SETD8 inhibitors.

Orthogonal SETD8 inhibitors
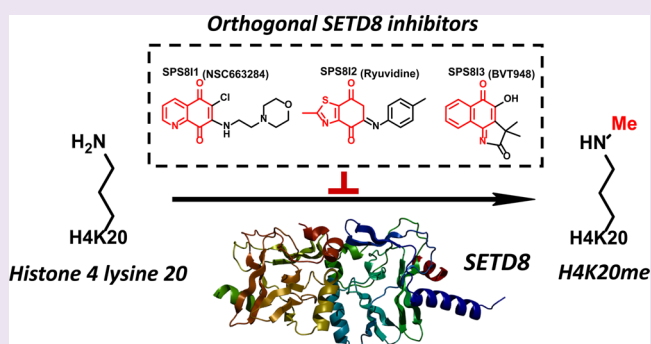
Proteome-wide methylation of lysine residues is an enzymatic posttranslational modification with multifaceted biological outcomes.[1,2] This process is catalyzed by protein lysine methyltransferases (PKMTs), which deposit the sulfonium methyl group of the cofactor *S*-adenosyl-L-methionine (SAM) on diverse histone and nonhistone targets.[1,2] Among more than 50 PKMTs encoded by the human genome, SETD8/SET8/Pr-SET7/KMT5A is the sole PKMT known for the *in vivo* monomethylation of histone H4 lysine 20 (H4K20me1).[3,4] The level of the SETD8 protein is finely tuned by multiple E3 ligases throughout a cell cycle with the highest level at G2/M phase and the lowest level at S phase.[4−9] Disruption of endogenous SETD8, accompanied by suppression of H4K20 monomethylation, leads to cell cycle defects, chromatin decondensation, and enlarged nuclei, indicating the essential role(s) of SETD8 in DNA replication.[10−13] SETD8 also methylates nonhistone targets such as proliferating cell nuclear antigen (PCNA), the tumor suppressor p53, and the p53-stabilizing factor Numb.[14−16] Methylation of p53 or Numb results in the downregulation of apoptosis either by antagonizing p53 acetylation, which is required for p53-mediated transcriptional activation, or promoting p53 ubiquitination for degradation.[14,15] These findings associate the functions of SETD8 with transcriptional regulation and DNA damage response. Inhibition of SETD8 is thus expected to show a proapoptotic phenotype through the depletion of H4K20 monomethylation, which leads to cell cycle arrest, or p53/Numb-mediated methylation, which results in the upregulation of p53 target genes.[14,15] SETD8 has been further implicated in cancer invasiveness and metastasis through its interaction with TWIST,[17] a master regulator in epithelial−mesenchymal transition.

The sheer scope of SETD8-associated biology highlights the importance of accessing SETD8 inhibitors, which enable convenient dissection of the functions of SETD8-mediated methylation. Despite such need, few inhibitors of high quality have been reported so far for SETD8 (also see Note),[18,19] as well as for other PKMTs implicated in epigenetics and disease.[20] Development of PKMT inhibitors aiming at both specificity and potency can be challenging because most PKMTs contain highly similar pockets for binding the SAM cofactor and less-structured regions for binding protein substrates.[20] A few examples of potent, selective PKMT inhibitors with demonstrated cellular activities include the chemical probes of G9a/GLP (e.g., UNC0638 and BRD4770), DOT1L (e.g., EPZ000477), and EZH1/2 (e.g., GSK126, EPZ-005687/6438 and EI1).[21−26] Prior efforts aimed at SETD8
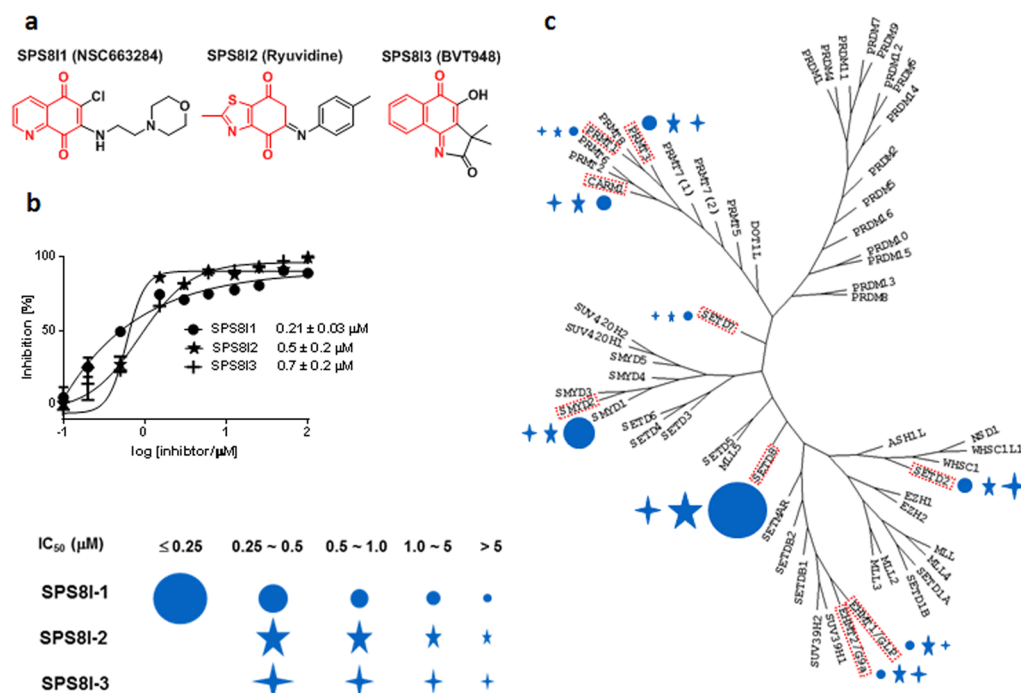
Figure 1. Chemical structures, *in vitro* IC$_{50}$, and selectivity of SETD8 inhibitors **SPS8I1−3**. (a) Chemical structures of the three HTS hits with quinonic moieties highlighted in red. **SPS8I1** (NSC663284), **SPS8I2** (ryuvidine), and **SPS8I3** (BVT948) were identified by HTS as potential SETD8 inhibitors and validated in the current work. (b) Dose−response curves of **SPS8I1−3**. The IC$_{50}$ values of **SPS8I1−3** against SETD8 were measured by the secondary filter paper assay using a low ratio of SAM/peptide/enzyme = 0.75:1.5:1 (see Supporting Information). (c) Selectivity of **SPS8I1−3** against a panel of PMTs. The magnitude of IC$_{50}$ values of **SPS8I1−3** is presented against nine phylogenetically related PMTs (their IC$_{50}$ values are listed in Supplementary Table S1). The diameters of symbols are proportional to the reciprocal values of IC$_{50}$ and thus higher potency of individual inhibitors. "●" for **SPS8I1**, "∗L" for **SPS8I2** and "+" for **SPS8I3**.

inhibition have also led to several compounds such as nahuoic acid A[18] and bis(bromo/dibromo-methoxylphenol) derivatives[19] as *in vitro* SETD8 inhibitors. However, these compounds have not demonstrated high selectivity or cellular activity against SETD8. The state of the field thus prompted us to explore other small-molecule scaffolds for SETD8 inhibition.

We recently formulated a radioactivity-based scintillation proximity imaging assay (SPA) in a high throughput screening (HTS) format with the purpose of identifying novel SETD8 inhibitors.[27] This assay relies on SETD8 to transfer the radioactive [3H-methyl] group from *S*-adenosyl-L-[3H-methyl]-methionine to a biotinylated H4K20 peptide substrate. The resultant radiolabeled peptide is immobilized onto steptavidin-conjugated SPA imaging polystyrene beads. The proximity between the β-emitting [3H-Me]-labeled peptide and the bead-coated scintillation fluid triggers a luminescence signal, which can be quantified using a LEADseeker system and is suppressed if SETD8 inhibitors are present in the methylation reaction. After screening >5000 compounds from commercial sources (e.g., MicroSource, Prestwick, Tocris, and Sigma), we identified 4 hits, which preferentially suppress the SPA signal of SETD8 but not those of SETD7, SETD2, and GLP (>50% inhibition at a concentration of 10 μM).[27] In the present work, we characterize these compounds and demonstrate that NSC663284, BVT948, and ryuvidine (3 out of the 4 HTS hits) inhibit SETD8 via different modes. NSC663284 (**SPS8I1**), ryuvidine (**SPS8I2**), and BVT948 (**SPS8I3**) efficiently and selectively suppress cellular H4K20me1 at doses lower than 5 μM within 24 h (see Figure 1a for the structures of **SPS8I1−3**). The cells treated with **SPS8I1−3** (Small-molecule Pool of SETD8 Inhibitor) recapitulate cell-

cycle-arrest phenotypes similar to what were reported for knocking down SETD8 by RNAi.[11] Given that the three compounds have distinct structures and inhibit SETD8 in different manners, they can be employed collectively as chemical genetic tools to interrogate SETD8-involved methylation.

Among the compounds identified in the SPA-based HTS assays of SETD8, SETD7, SETD2, and GLP, we focused on validating the 4 compounds that were identified solely in the HTS of SETD8.[27] The dose−response curves of these compounds against SETD8 were determined by a secondary radiometric filter paper assay.[27] Here, the assay parameters including the concentrations of [3H-methyl]-SAM, the H4K20 peptide substrate, and SETD8 (a low ratio of SAM/peptide/enzyme = 0.75:1.5:1) are similar to those used in the primary SPA-based HTS (see Supporting Information). Three compounds (**SPS8I1−3**) were confirmed as potent inhibitors of SETD8 with apparent IC$_{50}$ values of 0.21 ± 0.03 μM, 0.5 ± 0.2 μM, and 0.7 ± 0.2 μM, respectively (NSC95397 was triaged because of its high IC$_{50}$ value of 82 μM) (Figure 1b). The IC$_{50}$ values largely reflect the interaction between SETD8 and the inhibitors because the concentrations of SAM (0.75 μM) and the H4K20 peptide (1.5 μM) in the assay are far below the values of $K_{m,SAM}$ and $K_{m,H4K20}$ (24 ± 1 μM and 125 ± 3 μM, respectively, as will be reported elsewhere). The $K_{m,H4K20}$ value is within 3-fold of that reported previously.[28] It is worth noting that the sub-μM IC$_{50}$ of **SPS8I1−3** may not fully reflect their potency because these values fall into the micromolar range of SETD8's concentration used in the assay and thus represent the lowest values that can be reliably measured under the current settings (see Supporting Information). In addition, the

a

Actions of inhibitors	SPS8I-1	SPS8I-2	SPS8I-3
In vitro IC$_{50}$ (μM)	0.21	0.5	0.7
SAM-dependence	No	No	Yes
Substrate-dependence	Yes	No	Yes
Slow on-set character	Yes	Yes	Yes
Irreversible character	Highly likely	Highly likely	Highly likely
k_{inact} (min^{-1})	0.022	0.017	0.027
K_i (μM)	17	2	10
Cellular EC$_{50}$ (μM)	< 5, single dose	< 1, single dose	< 5, single dose
Cell-cycle arrest phenotype	S-phase in Day 1, then G2/M in Day 2	S-phase in Day 1 & Day 2	S-phase in Day 1, then G2/M in Day 2
Other PMT targets	SMYD2	unknown	PRMT3, SETD2 & CARM1
Cellular off-targets (Ref 32-37)	Cdc25	CDK2 & CDK4	PTPs

Figure 2. Characterization and comparison of SETD8 inhibition by **SPS8I1−3**. (a) Comparison of **SPS8I1−3** as SETD8 inhibitors *in vitro* and in a cellular setting. The IC$_{50}$ values of **SPS8I1−3** were extracted from Figure 1b. The inhibition modes for **SPS8I1−3** (SAM dependence, substrate dependence, slow onset/irreversible characters) were summarized according to the data in panels b−e. Values of k_{inact} and K_i were extracted from Supplementary Figure S1. The EC$_{50}$ values and cellular phenotypes of **SPS8I1−3** are summarized according to the data in Figure 3. The off-target effects of **SPS8I1−3** on other PMTs were based on the data in Figure 1c. The bottom line lists the reported non-PMT targets of **SPS8I1−3**.[33−38] (b,c) Characterization of SAM-dependent inhibition of SETD8 by **SPS8I1−3**. Relative IC$_{50}$ values were defined as the ratios of IC$_{50}$ values for each inhibitor (the concentration range of 0.1−100 μM was examined) in the presence of the varied concentrations of the SAM cofactor or substrate in the presence of the lowest concentration of SAM (1 μM) or substrate (5 μM), respectively. These numbers were then plotted against the ratios of [SAM]/$K_{m,SAM}$ or [substrate]/$K_{m,H4K20}$ ($K_{m,SAM}$ = 24 ± 1 μM and $K_{m,H4K20}$ or $K_{m,pep}$ = 125 ± 3 μM, as will be reported elsewhere), respectively. The data were arbitrarily fit to 0−3 order exponential curves to show a general trend of IC$_{50}$ versus the concentrations of SAM or H4K20 peptide. (d) Time-dependent, slow onset inactivation of SETD8 by **SPS8I1−3**. After incubating with the inhibitors, the relative methyltransferase activity of SETD8 was evaluated by measuring the initial rate and then plotted as the percentage of the loss of the activity versus the DMSO-treated control at different time intervals. (e) Irreversible character of SETD8 inhibition by **SPS8I1−3**. After preincubating **SPS8I1−3** to inactivate SETD8, the mixtures of SETD8 and inhibitors were diluted by 200-fold to lower the concentrations of inhibitors below their IC$_{50}$ values. The residual methyltransferase activity was monitored and presented as the percentage of the DMSO-treated control.

apparent *in vitro* IC$_{50}$ values of **SPS8I1−3** may alter according to the assay parameters such as the concentrations of reactants and preincubation/reaction time (see discussion later) and the unknown ratio of active versus misfolded SETD8 used in the assay.

To evaluate the selectivity of **SPS8I1−3** on SETD8 versus other PMTs, dose−response curves of these compounds were compared among a phylogenic panel of representative human methyltransferases, including 6 PKMTs (SETD2, GLP, G9a, SETD8, SMYD2, and SETD7) and 3 protein arginine methyltransferases (CARM1, PRMT1, and PRMT3) (Figure 1c; Supplmentary Tables S1 and S2). According to the 3 × 9 array of IC$_{50}$ values, **SPS8I1** (see discussion for its non-PMT targets) was identified as the most potent and selective SETD8 inhibitor with an apparent IC$_{50}$ of 0.21 ± 0.03 μM for SETD8, which is 2.5-fold lower than that of its next hit SMYD2 (0.5 ±
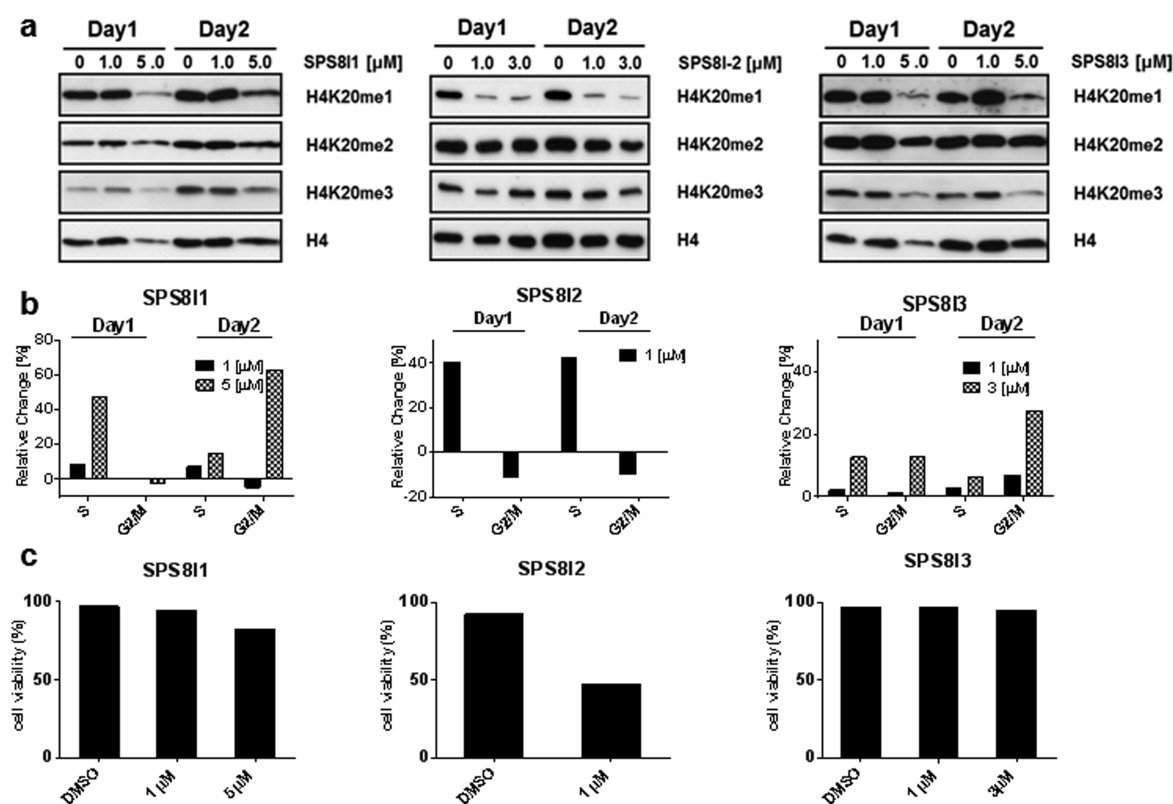
Figure 3. Cellular inhibition of SETD8 by **SPS8I1−3**. (a) Western blot of the H4K20me mark upon treatment with **SPS8I1−3**. The HEK293T cells were treated with varied concentrations of **SPS8I1−3** for 3 days (see Supplementary Figure S5 for Day 3). The level of H4K20me was examined as a cellular mark of SETD8's methyltransferase activity with the levels of H4 and H4K20me2/3 as controls. (b) Cell cycle arrest phenotype associated with **SPS8I1−3**. HEK293T cells were treated with varied concentrations of **SPS8I1−3** for 3 days. The cell cycle distributions of the treated cells were analyzed by flow cytometry. The distributions of cells in S phase and G2/M phase were plotted as their percentage changes in comparison with the DMSO-treated controls. (c) Viability of HEK293T cells treated with **SPS8I1−3**. HEK293T cells were treated with the varied concentrations of **SPS8I1−3** for 3 days. Cell viability was determined by trypan blue staining with the DMSO-treated cells as the controls. Here the cells were treated with 0, 1, and 5 μM of **SPS8I1** (left panel); 0 and 1 μM of **SPS8I2** (central panel); 0, 1, and 3 μM of **SPS8I3** (right panel).

0.2 μM) and >6-fold lower than those of other examined PMTs (from 1.3 to >100 μM) (Figure 1c and Supplementary Table S1). With the 2.5-fold ratio of IC_{50} values as a threshold, **SPS8I2** also demonstrates desired selectivity for SETD8 versus other examined PMTs (Figure 1c and Supplementary Table S1). In contrast, **SPS8I3** shows modest selectivity with potential cross-inhibition against PRMT3, SETD2, and CARM1 (Figure 1c and Supplementary Table S1). In a collective view, although the individual **SPS8I1−3** might hit multiple PMTs as well as other cellular targets (see discussion later), all three compounds act on SETD8 as the commonly shared PMT target (Figures 1e, 2a).

Given that **SPS8I1−3** are structurally distinct except for their quinonic moiety (Figure 1a, highlighted in red), we reasoned that they may act on SETD8 differently (e.g., dependence on cofactor or substrate). Inhibition of SETD8 by **SPS8I1−3** was thus examined by measuring relative IC_{50} values of each inhibitor as a function of the ratios of the concentrations of SAM and the H4K20 peptide substrate versus their respective K_m values (Figure 2b,c). SETD8 inhibition mediated by the three compounds (**SPS8I1−3**) shows a different behavior toward the SAM cofactor with a SAM-dependent character for **SPS8I3** (the presence of SAM facilitates SETD8 inhibition) versus a SAM-independent character for **SPS8I1** and **SPS8I2** (Figure 2b). Concomitantly, **SPS8I1** and **SPS8I3** are substrate-dependent inhibitors, as shown by the increased IC_{50} values in the presence of high concentration of substrate, while **SPS8I2** is

a substrate-independent inhibitor (Figure 2c). Collectively, the three compounds display different characters for SETD8 inhibition within the examined concentrations of SAM and H4K20 peptide, with **SPS8I1** favoring the absence of substrate while being insensitive to the presence of SAM, **SPS8I3** favoring the absence of substrate and the presence of SAM, and **SPS8I2** insensitive to the presence of both SAM and substrate (Figure 2a). Although it is of our interest to explore whether the same trend can be followed within a broader range of concentrations of SAM and the H4K20 peptide (e.g., under saturation conditions), the high K_m values (24 μM for SAM and 125 μM for peptide substrate) make it challenging to design such experiments.

Given that **SPS8I1−3** share a quinonic motif (Figure 1a) and may act on reactive Cys residues by forming covalent adducts as implicated elsewhere,[29] we examined the mechanism of SETD8 inhibition by **SPS8I1−3**. Incubation of **SPS8I1−3** causes a time-dependent inactivation of SETD8's methyltransferase activity (Figure 2d; Supporting Information). SETD8 inhibition, once achieved by **SPS8I1−3**, can be sustained over a long period of time (at least 20 h, Figure 2e) even after diluting out free inhibitors (Supporting Information). In contrast, DMSO-treated SETD8 is fully active during the period of incubation (Figure 2d). Given the irreversible character of **SPS8I1−3**-mediated SETD8 inhibition, we further measured their k_{inact}/K_i values through time-dependent progression. The k_{inact} values of 0.017−0.027 min^{-1} and the K_i values of 2−17

μM indicate that **SPS8I1−3** inhibit SETD8 via an irreversible, slow onset process (Figure 2a, Supplementary Figure S1). As preliminary structure−activity relationship analysis, we also collected three commercial available compounds whose structures contain a quinonic motif and are related to **SPS8I1−3** (Supplementary Table S3). All of these compounds are inert to SETD8 inhibition (Supplementary Table S3), suggesting that **SPS8I1−3**'s special structures rather than the general quinonic motif are essential for SETD8 inhibition.

Structural alignment of the 6 PKMTs examined in the current work (Figure 1c, Supplementary Figure S2a) highlights that SETD8 and SMYD2 contain a distinct Cys residue (Cys270 for SETD8 and Cys181 for SMYD2) around their active sites (Supplementary Figure S2a). Given that **SPS8I1** inhibits both SETD8 and SMYD2 (IC_{50} = 0.21 μM and 0.5 μM, Figure 1c, Supplementary Table S1), we examined whether SETD8's Cys270 is the target residue to form potential covalent adducts for the observed inhibition. Remarkably, SETD8's C270S mutant is around 10-fold more resistant to the inhibition of **SPS8I1** and **SPS8I2** (Supplementary Figure S2b,c) and shows different Hill coefficients in comparison with native SETD8 (Supplementary Figure S2b−d). In contrast, **SPS8I3** equally inhibits native SETD8 and the C270S variant (Supplementary Figure S2d). SETD8's C270 was thus identified as the relevant site for **SPS8I1** and **SPS8I2** to form covalent adducts, while **SPS8I3** may target Cys residues in a more general manner. The different modes of inhibition of **SPS8I1−3** may rationalize the modest selectivity of **SPS8I3** (SETD8, PRMT3, SETD2, and CARM1 in Figure 1c and Supplementary Table S1) versus the higher specificity of **SPS8I1** and **SPS8I2** (SETD2 and SMYD2 in Figure 1c and Supplementary Table S1). Here we further performed a Differential Scanning Fluorimetry (DSF) assay to examine inhibitor-bound SETD8. The remarkable thermal shift of 3−6 °C with SYPRO Orange staining for **SPS8I1-3** suggests that the SETD8-inhibitor adducts are more susceptible to thermal denaturation and likely adopt less stable, catalytic-inactive conformations (Supplementary Figure S3). In contrast, no such thermal shift was observed for **SPS8I1** and **SPS8I2** against SETD8's C270S mutant (Supplementary Figure S3). The collective evidence thus argues that **SPS8I1−3** are selective and irreversible inhibitors of SETD8 with distinct structures and at least two modes of interaction (Figure 2a). It remains interesting to solve the structure of the inhibitor-bound SETD8 to further elucidate the mode of interaction.

The irreversible character of **SPS8I1−3**, together with their different dependence on SAM and substrate for SETD8 inhibition, makes it challenging to evaluate these compounds solely by their *in vitro* IC_{50} (or K_d values). We therefore examined the efficiency of **SPS8I1−3** by their ability to suppress SETD8's methylation mark, H4K20me1, under a cellular setting. After treating HEK293T cells with **SPS8I1−3**, H4K20me1 was rapidly depleted within 24 h, and this effect can be sustained for 3 days with a single -dose of 5 μM **SPS8I1**, 1 μM **SPS8I2**, or 5 μM **SPS8I3** (Figure 3a; Supplementary Figures S4 and S5). H4K20me1 remained low within 24 h after the treatment with the three inhibitors, indicating that **SPS8I1−3** are potent SETD8 inhibitors in the cellular setting. In contrast, no significant change was observed for control marks such as total H4, H4K20me2/3, H3, and H3K9me (Figure 3a; Supplementary Figures S4a, S5). This conclusion was further enforced by quantifying the relative ratios of H4K20me and H4K20me2/3 versus H4 (Supplementary

Figure S4b). Because the cells cannot sustain the treatment longer than 3 days (data not shown), we did not further examine other histone marks such as H3K9me2/3, H3K27me2/3, and H3K79me2/3, whose depletion generally takes at least 4 days.[23,24] Here the time course of the H4K20me1 depletion is consistent with a previous observation that H4K20me1 is a dynamic histone mark and subject to rapid methylation to H4K20me2/3 by SUV420H1/2.[13,30−32] The pool of H4K20me1 can be depleted by blocking its production by **SPS8I1−3**, coupled with its rapid conversion to H4K20me2/3 by SUV420H1/2. For the cells treated with **SPS8I1−3**, we also noted a residual level of H4K20me1, which might arise from the H4K20me intermediate during the production of H4K20me2/3 by SUV420H1/2 rather than insufficient inhibition of SETD8 as also observed elsewhere (Figure 3a).[13] Collectively, these results demonstrated the efficiency of **SPS8I1−3** to inhibit SETD8 under a cellular setting, accompanied by rapid depletion of H4K20me1, at a single dose of 1−5 μM (Figure 2a).

After validating the efficiency of SETD8 inhibition by **SPS8I1−3** *in vitro* and in a cellular setting, we further examined the cell-cycle phenotype associated with the treatment of these compounds. Several prior efforts have showed that RNAi-mediated knockdown of SETD8 results in cell-cycle defects at S phase and G_2/M phase.[11,13] These phenotypes can also be recapitulated by knocking in catalytically dead SETD8 as a dominant-negative mutant.[11] After treating HEK293T cells with **SPS8I1** at a single subtoxic dose of 5 μM (see viability in Figure 3c), a significant portion of cells were accumulated at S phase after 24 h in comparison with the controls (DMSO or a less effective dose of 1 μM) (Figure 3b, Supplementary Figure S6). The S phase delay was released after 24 h accompanied by increased accumulation of the cells at G2/M phase (Figure 3b, Supplementary Figure S6). A similar phenotype (an increased population of S-phase at 24 h and then an increased population of G2/M phase within 48 h) was also observed upon treating the cells with **SPS8I3** at a single dose of 3 μM (Figure 3b, right panel). It is worth noting that the phenotype for **SPS8I3** slightly differs from that of **SPS8I1** with a more rapid G2/M accumulation for the latter by 24 h. Treating HEK293T cells with **SPS8I2** at a single dose of 1 μM also caused S-phase accumulation, although the S-phase arrest was sustained for at least 48 h and did not proceed to G2/M phase as observed for **SPS8I1** and **SPS8I3** (Figure 3b, middle panel). The slightly different phenotypes of cell cycle defects observed for **SPS8I1−3** were likely caused by respective off-target effects (see later discussion). The minimal dosage (1−5 μM **SPS8I1−3**) and the short treatment period (24 h) required for the manifestation of the cell-cycle defects correlate well with the dose-dependent depletion of SETD8's methylation mark H4K20me1 (Figure 3a versus b). Such consistency argues that SETD8 inhibition and cell-cycle arrest occur in a comparable time frame upon exposing cells to these inhibitors. The cell-cycle defects were apparently not caused by depleting other histone marks such as H3K9me1/2/3, H3K27me2/3, and H3K79me2/3, a process that generally takes longer than 3 days.[23,24] **SPS8I1−3**-associated cell-cycle defects are also unlikely due to general toxicity, given that >50% cells are still viable under these doses (Figure 3c versus Figure 3a,b).

The screening of **SPS8I1−3** against the panel of PMTs revealed potential off-target effects on other PMTs (**SPS8I1** for SMYD2 and **SPS8I3** for PRMT3 and SETD2, Figure 1c). Other cellular targets of **SPS8I1−3** were also documented

previously in PMT-unrelated settings. For instance, **SPS8I1** (NSC663284) was reported as an inhibitor of Cdc25, a dual specificity phosphatase.[33−35] The inhibition of Cdc25 by **SPS8I1** (NSC663284) was proposed to occur via the production of a covalent adduct or the generation of reactive oxygen species (ROS). For the former mechanism, the catalytic domain of Cdc25 is expected to be inactivated by a 1,4-Michael addition of a serine residue adjacent to the catalytic cysteine. For the latter mechanism, the quinone moiety of this compound may facilitate the oxidation of Cdc25's catalytic cysteine by the formation of ROS via reductive-oxidative cycling under a cellular context.[34] Similarly, **SPS8I3** was reported to inhibit several protein tyrosine phosphatases PTPs (e.g., PTP1B) via the production of ROS, such as hydrogen peroxide, and the oxidation of the PTPs' catalytic cysteines under a cellular setting.[36,37] **SPS8I2** was documented as an *in vitro* inhibitor of cyclin-dependent kinase 4 and 2 (CDK4/2).[38] The off-target effect of **SPS8I2** as a CDK2/4 inhibitor may rationalize the severe S-phase defect associated with this compound (Figure 3b).

Nahuoic acid A and bis(bromo/dibromo-methoxylphenol) derivatives were reported previously as SETD8 inhibitors, despite no demonstration of cellular activity for the former and the lack of SETD8 selectivity for the latter.[18,19] Interestingly, both of the compounds contain the structural motifs that are amenable for 1,4-Michael addition for reactive Cys residues. Similarly, **SPS8I1**, **SPS8I2**, and **SPS8I3** contain a quinone moiety, which can also be subject to 1,4-Michael addition of reactive Cys residues such as SET8's Cys270 for **SPS8I1** and **SPS8I2** and thus irreversibly inhibit SETD8. The commonality of the reactive functional groups in **SPS8I1−3**, Nahuoic acid A, and bis(bromo/dibromo-methoxylphenol) derivatives suggests that SETD8 may contain reactive Cys residues such as Cys270 that potentially react with **SPS8I1−3** for the observed inhibition. Here we also ruled out the possibility that **SPS8I1−3** inhibit SETD8's methyltransferase activity through their general redox potential for the following reasons: (a) **SPS8I1** and **SPS8I2** are inert toward SETD8's C270S mutant, arguing that the inhibitors act on SETD8 by selectively targeting this Cys residue; (b) several structurally related compounds, though containing the redox-active quinonic motif, are inert toward SETD8 (Supplementary Table S3).

SETD8 is the sole PKMT known for H4K20 monomethylation (H4K20me1) *in vivo*.[3,4] H4K20me1 can be either removed by PHF8 or methylated to H4K20me2/3 with a half-lifetime of a few hours.[4,13,30−32,39] The dynamic character for H4K20me1 was well reflected by its rapid depletion by **SPS8I1−3** within 24 h, in contrast to the more stable histone methylation marks such as H3K9me2/3, H3K27me2/3, and H3K79me2/3.[23,24] A residual level of H4K20me1 after the treatment with **SPS8I1−3** (Figure 3a) may arise from the incomplete production of H4K20me2/3 by SUV240H1/2.[13] In contrast to the dramatic decrease of the H4K20me1 mark upon the treatment with **SPS8I1−3**, no acute change of the H4K20me2/3 marks was observed, although H4K20me1 has been implicated as SUV420H1/2's substrate for H4K20me2/3 production.[13] This observation suggests that H4K20me2/3, like H3K9me2/3, H3K27me2/3, and H3K79me2/3, are more stable histone methylation marks, and the 1−3-day depletion of H4K20me1 (<5% of the overall methylated H4K20) has a limited impact on overall H4K20me2/3 levels (>95% of the overall methylated H4K20).[13,30−32] Besides the H4K20me1 depletion, **SPS8I−**treated HEK293T cells display cell cycle

defects at S phase within 24 h, suggesting that this phenotype is associated with the depletion of H4K20me1 mark but not H4K20me2/3, whose levels remain largely unchanged during the period of treatment. The cell cycle defect can then proceed to G2/M phase within 24−48 h as demonstrated by **SPS8I1** and **SPS8I3**. These results argue that the S phase delay caused by SETD8 inhibition is transient and can eventually advance to G2/M arrest. More importantly, these phenotypes tightly correlate with the H4K20me1 mark and SETD8's methyltransferase activity. Interestingly, both S-phase and G2/M-phase defects were reported previously as the phenotypes of SETD8 knockdown.[11,40] Such discrepancy (S-phase versus G2/M-phase defect) can be rationalized by the different time frames of SETD8 knockdown in individual experimental settings.

In the current work, 3 out of 4 HTS hits were validated *in vitro* and in a cellular context as potent inhibitors of SETD8. This hit validation rate is remarkable and underscores the robustness of the SPA-based HTS assay for identifying SETD8 inhibitors. The general applicability of the SPA-based HTS assay also highlights its merits for screening other PMTs.[27] The 3 compounds were characterized as potent inhibitors of SETD8 with the ability to suppress SETD8's H4K20me1 mark at single doses of 1−5 μM in a cellular context. Structurally distinct **SPS8I1−3** also display different modes of SETD8 inhibition. Such differences also make **SPS8I1−3** less likely to act on other common cellular targets besides SETD8. As a result, the shared phenotypes of the 3 compounds are expected to be associated with SETD8 inhibition. More importantly, at the effective doses required for H4K20me1 suppression, the observed cell-cycle-arrest phenotype of **SPS8I1−3** is similar to that observed for SETD8 knockdown.[11] Strikingly, the phenotypes of the H4K20me1 depletion and cell cycle arrest of **SPS8I1−3** can be sustained for up to 3 days at a single dose of <5 μM **SPS8I1−3**. Such robust inhibition of SETD8 by **SPS8I1−3**, together with their different off-target effects, argues that these compounds can be used collectively as SETD8 inhibitors to offset off-target effects of individual reagents. At this stage, we envision using all three compounds to examine SETD8 inhibition and then focusing on the phenotypes shared by all of them. **SPS8I1** and **SPS8I2** were reported to be cytotoxic toward various cancer cell lines.[35,38] Given the general cell cycle arrest phenotypes of **SPS8I1−3**, as well as the specific implication in cancer,[14,15,17,35,38] it is of great interest to further examine these compounds and their derivatives for more selective SETD8 inhibitors and novel anticancer reagents.

■ METHODS

See Supporting Information.

■ ASSOCIATED CONTENT

Ⓢ Supporting Information

Supplementary figures and tables, materials and methods. This material is available free of charge via the Internet at http://pubs.acs.org.

■ AUTHOR INFORMATION

Corresponding Author

*E-mail: luom@mskcc.org.

Author Contributions

⊥These authors contributed equally to this work.

Notes

■ ACKNOWLEDGMENTS

■ REFERENCES

(1) Kouzarides, T. (2007) Chromatin modifications and their function. *Cell 128*, 693−705.

(2) Luo, M. (2012) Current chemical biology approaches to interrogate protein methyltransferases. *ACS Chem. Biol. 7*, 443−463.

(3) Nishioka, K., Rice, J. C., Sarma, K., Erdjument-Bromage, H., Werner, J., Wang, Y., Chuikov, S., Valenzuela, P., Tempst, P., Steward, R., Lis, J. T., Allis, C. D., and Reinberg, D. (2002) PR-Set7 is a nucleosome-specific methyltransferase that modifies lysine 20 of histone H4 and is associated with silent chromatin. *Mol. Cell 9*, 1201−1213.

(4) Wu, S., and Rice, J. C. (2011) A new regulator of the cell cycle: the PR-Set7 histone methyltransferase. *Cell Cycle 10*, 68−72.

(5) Jorgensen, S., Eskildsen, M., Fugger, K., Hansen, L., Larsen, M. S., Kousholt, A. N., Syljuasen, R. G., Trelle, M. B., Jensen, O. N., Helin, K., and Sorensen, C. S. (2011) SET8 is degraded via PCNA-coupled CRL4(CDT2) ubiquitylation in S phase and after UV irradiation. *J. Cell. Biol. 192*, 43−54.

(6) Centore, R. C., Havens, C. G., Manning, A. L., Li, J. M., Flynn, R. L., Tse, A., Jin, J., Dyson, N. J., Walter, J. C., and Zou, L. (2010) CRL4(Cdt2)-mediated destruction of the histone methyltransferase Set8 prevents premature chromatin compaction in S phase. *Mol. Cell 40*, 22−33.

(7) Oda, H., Hubner, M. R., Beck, D. B., Vermeulen, M., Hurwitz, J., Spector, D. L., and Reinberg, D. (2010) Regulation of the histone H4 monomethylase PR-Set7 by CRL4(Cdt2)-mediated PCNA-dependent degradation during DNA damage. *Mol. Cell 40*, 364−376.

(8) Wu, S., Wang, W., Kong, X., Congdon, L. M., Yokomori, K., Kirschner, M. W., and Rice, J. C. (2010) Dynamic regulation of the PR-Set7 histone methyltransferase is required for normal cell cycle progression. *Genes Dev. 24*, 2531−2542.

(9) Abbas, T., Shibata, E., Park, J., Jha, S., Karnani, N., and Dutta, A. (2010) CRL4(Cdt2) regulates cell proliferation and histone gene expression by targeting PR-Set7/Set8 for degradation. *Mol. Cell 40*, 9−21.

(10) Huen, M. S., Sy, S. M., van Deursen, J. M., and Chen, J. (2008) Direct interaction between SET8 and proliferating cell nuclear antigen couples H4-K20 methylation with DNA replication. *J. Biol. Chem. 283*, 11073−11077.

(11) Houston, S. I., McManus, K. J., Adams, M. M., Sims, J. K., Carpenter, P. B., Hendzel, M. J., and Rice, J. C. (2008) Catalytic function of the PR-Set7 histone H4 lysine 20 monomethyltransferase is essential for mitotic entry and genomic stability. *J. Biol. Chem. 283*, 19478−19488.

(12) Tardat, M., Brustel, J., Kirsh, O., Lefevbre, C., Callanan, M., Sardet, C., and Julien, E. (2010) The histone H4 Lys 20 methyltransferase PR-Set7 regulates replication origins in mammalian cells. *Nat. Cell Biol. 12*, 1086−1093.

(13) Jorgensen, S., Schotta, G., and Sorensen, C. S. (2013) Histone H4 lysine 20 methylation: key player in epigenetic regulation of genomic integrity. *Nucleic Acids Res. 41*, 2797−2806.

(14) Shi, X., Kachirskaia, I., Yamaguchi, H., West, L. E., Wen, H., Wang, E. W., Dutta, S., Appella, E., and Gozani, O. (2007) Modulation of p53 function by SET8-mediated methylation at lysine 382. *Mol. Cell 27*, 636−646.

(15) Dhami, G. K., Liu, H., Galka, M., Voss, C., Wei, R., Muranko, K., Kaneko, T., Cregan, S. P., Li, L., and Li, S. S. (2013) Dynamic methylation of Numb by Set8 regulates its binding to p53 and apoptosis. *Mol. Cell 50*, 565−576.

(16) Takawa, M., Cho, H. S., Hayami, S., Toyokawa, G., Kogure, M., Yamane, Y., Iwai, Y., Maejima, K., Ueda, K., Masuda, A., Dohmae, N., Field, H. I., Tsunoda, T., Kobayashi, T., Akasu, T., Sugiyama, M., Ohnuma, S., Atomi, Y., Ponder, B. A., Nakamura, Y., and Hamamoto, R. (2012) Histone lysine methyltransferase SETD8 promotes carcinogenesis by deregulating PCNA expression. *Cancer Res. 72*, 3217−3227.

(17) Yang, F., Sun, L., Li, Q., Han, X., Lei, L., Zhang, H., and Shang, Y. (2012) SET8 promotes epithelial-mesenchymal transition and confers TWIST dual transcriptional activities. *EMBO J. 31*, 110−123.

(18) Williams, D. E., Dalisay, D. S., Li, F., Amphlett, J., Maneerat, W., Chavez, M. A., Wang, Y. A., Matainaho, T., Yu, W., Brown, P. J., Arrowsmith, C. H., Vedadi, M., and Andersen, R. J. (2013) Nahuoic acid A produced by a Streptomyces sp. isolated from a marine sediment is a selective SAM-competitive inhibitor of the histone methyltransferase SETD8. *Org. Lett. 15*, 414−417.

(19) Valente, S., Lepore, I., Dell'Aversana, C., Tardugno, M., Castellano, S., Sbardella, G., Tomassi, S., Di Maro, S., Novellino, E., Di Santo, R., Costi, R., Altucci, L., and Mai, A. (2012) Identification of PR-SET7 and EZH2 selective inhibitors inducing cell death in human leukemia U937 cells. *Biochimie 94*, 2308−2313.

(20) Copeland, R. A., Solomon, M. E., and Richon, V. M. (2009) Protein methyltransferases as a target class for drug discovery. *Nat. Rev. Drug Discovery 8*, 724−732.

(21) Yuan, Y., Wang, Q., Paulk, J., Kubicek, S., Kemp, M. M., Adams, D. J., Shamji, A. F., Wagner, B. K., and Schreiber, S. L. (2012) A small-molecule probe of the histone methyltransferase G9a induces cellular senescence in pancreatic adenocarcinoma. *ACS Chem. Biol. 7*, 1152−1157.

(22) Daigle, S. R., Olhava, E. J., Therkelsen, C. A., Majer, C. R., Sneeringer, C. J., Song, J., Johnston, L. D., Scott, M. P., Smith, J. J., Xiao, Y., Jin, L., Kuntz, K. W., Chesworth, R., Moyer, M. P., Bernt, K. M., Tseng, J. C., Kung, A. L., Armstrong, S. A., Copeland, R. A., Richon, V. M., and Pollock, R. M. (2011) Selective killing of mixed lineage leukemia cells by a potent small-molecule DOT1L inhibitor. *Cancer Cell 20*, 53−65.

(23) McCabe, M. T., Ott, H. M., Ganji, G., Korenchuk, S., Thompson, C., Van Aller, G. S., Liu, Y., Graves, A. P., Della Pietra, A., 3rd, Diaz, E., LaFrance, L. V., Mellinger, M., Duquenne, C., Tian, X., Kruger, R. G., McHugh, C. F., Brandt, M., Miller, W. H., Dhanak, D., Verma, S. K., Tummino, P. J., and Creasy, C. L. (2012) EZH2 inhibition as a therapeutic strategy for lymphoma with EZH2-activating mutations. *Nature 492*, 108−112.

(24) Vedadi, M., Barsyte-Lovejoy, D., Liu, F., Rival-Gervier, S., Allali-Hassani, A., Labrie, V., Wigle, T. J., Dimaggio, P. A., Wasney, G. A., Siarheyeva, A., Dong, A., Tempel, W., Wang, S. C., Chen, X., Chau, I., Mangano, T. J., Huang, X. P., Simpson, C. D., Pattenden, S. G., Norris, J. L., Kireev, D. B., Tripathy, A., Edwards, A., Roth, B. L., Janzen, W. P., Garcia, B. A., Petronis, A., Ellis, J., Brown, P. J., Frye, S. V., Arrowsmith, C. H., and Jin, J. (2011) A chemical probe selectively inhibits G9a and GLP methyltransferase activity in cells. *Nat. Chem. Biol. 7*, 566−574.

2477

dx.doi.org/10.1021/cb500515r | *ACS Chem. Biol.* 2014, 9, 2471−2478

(25) Knutson, S. K., Kawano, S., Minoshima, Y., Warholic, N. M., Huang, K. C., Xiao, Y., Kadowaki, T., Uesugi, M., Kuznetsov, G., Kumar, N., Wigle, T. J., Klaus, C. R., Allain, C. J., Raimondi, A., Waters, N. J., Smith, J. J., Porter-Scott, M., Chesworth, R., Moyer, M. P., Copeland, R. A., Richon, V. M., Uenaka, T., Pollock, R., Kuntz, K. W., Yokoi, A., and Keilhack, H. (2014) Selective inhibition of EZH2 by EPZ-6438 leads to potent antitumor activity in *EZH2*-mutant non-Hodgkin lymphoma. *Mol. Cancer Ther. 13*, 842−854.

(26) Qi, W., Chan, H., Teng, L., Li, L., Chuai, S., Zhang, R., Zeng, J., Li, M., Fan, H., Lin, Y., Gu, J., Ardayfio, O., Zhang, J. H., Yan, X., Fang, J., Mi, Y., Zhang, M., Zhou, T., Feng, G., Chen, Z., Li, G., Yang, T., Zhao, K., Liu, X., Yu, Z., Lu, C. X., Atadja, P., and Li, E. (2012) Selective inhibition of Ezh2 by a small molecule inhibitor blocks tumor cells proliferation. *Proc. Natl. Acad. Sci. U.S.A. 109*, 21360−21365.

(27) Ibanez, G., Shum, D., Blum, G., Bhinder, B., Radu, C., Antczak, C., Luo, M., and Djaballah, H. (2012) A high throughput scintillation proximity imaging assay for protein methyltransferases. *Comb. Chem. High Throughput Screening 15*, 359−371.

(28) Couture, J. F., Collazo, E., Brunzelle, J. S., and Trievel, R. C. (2005) Structural and functional analysis of SET8, a histone H4 Lys-20 methyltransferase. *Genes Dev. 19*, 1455−1465.

(29) Kar, S., Lefterov, I. M., Wang, M., Lazo, J. S., Scott, C. N., Wilcox, C. S., and Carr, B. I. (2003) Binding and inhibition of Cdc25 phosphatases by vitamin K analogues. *Biochemistry 42*, 10490−10497.

(30) Oda, H., Okamoto, I., Murphy, N., Chu, J., Price, S. M., Shen, M. M., Torres-Padilla, M. E., Heard, E., and Reinberg, D. (2009) Monomethylation of histone H4-lysine 20 is involved in chromosome structure and stability and is essential for mouse development. *Mol. Cell. Biol. 29*, 2278−2295.

(31) Pesavento, J. J., Yang, H., Kelleher, N. L., and Mizzen, C. A. (2008) Certain and progressive methylation of histone H4 at lysine 20 during the cell cycle. *Mol. Cell. Biol. 28*, 468−486.

(32) Zee, B. M., Levin, R. S., Dimaggio, P. A., and Garcia, B. A. (2010) Global turnover of histone post-translational modifications and variants in human cells. *Epigenet. Chromatin 3*, 22.

(33) Pu, L., Amoscato, A. A., Bier, M. E., and Lazo, J. S. (2002) Dual G1 and G2 phase inhibition by a novel, selective Cdc25 inhibitor 6-chloro-7-[corrected](2-morpholin-4-ylethylamino)-quinoline-5,8-dione. *J. Biol. Chem. 277*, 46877−46885.

(34) Brisson, M., Nguyen, T., Wipf, P., Joo, B., Day, B. W., Skoko, J. S., Schreiber, E. M., Foster, C., Bansal, P., and Lazo, J. S. (2005) Redox regulation of Cdc25B by cell-active quinolinediones. *Mol. Pharmacol. 68*, 1810−1820.

(35) Lazo, J. S., Aslan, D. C., Southwick, E. C., Cooley, K. A., Ducruet, A. P., Joo, B., Vogt, A., and Wipf, P. (2001) Discovery and biological evaluation of a new family of potent inhibitors of the dual specificity protein phosphatase Cdc25. *J. Med. Chem. 44*, 4042−4049.

(36) Han, Y., Shen, H., Carr, B. I., Wipf, P., Lazo, J. S., and Pan, S. S. (2004) NAD(P)H:quinone oxidoreductase-1-dependent and -independent cytotoxicity of potent quinone Cdc25 phosphatase inhibitors. *J. Pharmacol. Exp. Ther. 309*, 64−70.

(37) Liljebris, C., Baranczewski, P., Bjorkstrand, E., Bystrom, S., Lundgren, B., Tjernberg, A., Warolen, M., and James, S. R. (2004) Oxidation of protein tyrosine phosphatases as a pharmaceutical mechanism of action: a study using 4-hydroxy-3,3-dimethyl-2H-benzo[g]indole-2,5(3H)-dione. *J. Pharmacol. Exp. Ther. 309*, 711−719.

(38) Ryu, C. K., Kang, H. Y., Lee, S. K., Nam, K. A., Hong, C. Y., Ko, W. G., and Lee, B. H. (2000) 5-Arylamino-2-methyl-4,7-dioxobenzothiazoles as inhibitors of cyclin-dependent kinase 4 and cytotoxic agents. *Bioorg. Med. Chem. Lett. 10*, 461−464.

(39) Liu, W., Tanasa, B., Tyurina, O. V., Zhou, T. Y., Gassmann, R., Liu, W. T., Ohgi, K. A., Benner, C., Garcia-Bassets, I., Aggarwal, A. K., Desai, A., Dorrestein, P. C., Glass, C. K., and Rosenfeld, M. G. (2010) PHF8 mediates histone H4 lysine 20 demethylation events involved in cell cycle progression. *Nature 466*, 508−512.

(40) Tardat, M., Murr, R., Herceg, Z., Sardet, C., and Julien, E. (2007) PR-Set7-dependent lysine methylation ensures genome replication and stability through S phase. *J. Cell. Biol. 179*, 1413−1426.

(41) Ma, A., Yu, W., Li, F., Bleich, R. M., Herold, J. M., Butler, K. V., Norris, J. L., Korboukh, V., Tripathy, A., Janzen, W. P., Arrowsmith, C. H., Frye, S. V., Vedadi, M., Brown, P. J., and Jin, J. (2014) Discovery of a selective, substrate-competitive inhibitor of the lysine methyltransferase SETD8. *J. Med. Chem. 57*, 6822−6833.